Free Radical Biology and Medicine 206 (2023) 134–142

Contents lists available at ScienceDirect

Free Radical Biology and Medicine

journal homepage: www.elsevier.com/locate/freeradbiomed

Oxygen-consumption based quantification of chemogenetic H_2O_2 production in live human cells

Wytze T.F. den Toom [a,2], Daan M.K. van Soest [a,2], Paulien E. Polderman [a], Miranda H. van Triest [a], Lucas J.M. Bruurs [a,1], Sasha De Henau [a], Boudewijn M.T. Burgering [a,b], Tobias B. Dansen [a,*]

[a] Center for Molecular Medicine, University Medical Center Utrecht, Universiteitsweg 100, 3584 CG, Utrecht, the Netherlands
[b] Oncode Institute, Jaarbeursplein 6, 3521 AL, Utrecht, the Netherlands

ARTICLE INFO

Keywords:
H_2O_2
D-amino acid oxidase
Oxygen consumption rate
HyPer7

ABSTRACT

Reactive Oxygen Species (ROS) in the form of H_2O_2 can act both as physiological signaling molecules as well as damaging agents, depending on their concentration and localization. The downstream biological effects of H_2O_2 were often studied making use of exogenously added H_2O_2, generally as a bolus and at supraphysiological levels. But this does not mimic the continuous, low levels of intracellular H_2O_2 production by for instance mitochondrial respiration. The enzyme D-Amino Acid Oxidase (DAAO) catalyzes H_2O_2 formation using D-amino acids, which are absent from culture media, as a substrate. Ectopic expression of DAAO has recently been used in several studies to produce inducible and titratable intracellular H_2O_2. However, a method to directly quantify the amount of H_2O_2 produced by DAAO has been lacking, making it difficult to assess whether observed phenotypes are the result of physiological or artificially high levels of H_2O_2. Here we describe a simple assay to directly quantify DAAO activity by measuring the oxygen consumed during H_2O_2 production. The oxygen consumption rate (OCR) of DAAO can directly be compared to the basal mitochondrial respiration in the same assay, to estimate whether the ensuing level of H_2O_2 production is within the range of physiological mitochondrial ROS production. In the tested monoclonal RPE1-hTERT cells, addition of 5 mM D-Ala to the culture media amounts to a DAAO-dependent OCR that surpasses ~5% of the OCR that stems from basal mitochondrial respiration and hence produces supra-physiological levels of H_2O_2. We show that the assay can also be used to select clones that express differentially localized DAAO with the same absolute level of H_2O_2 production to be able to discriminate the effects of H_2O_2 production at different subcellular locations from differences in total oxidative burden. This method therefore greatly improves the interpretation and applicability of DAAO-based models, thereby moving the redox biology field forward.

1. Introduction

H_2O_2 is produced endogenously at several subcellular locations, either directly or indirectly as the more reactive superoxide anion ($O_2^{\bullet-}$) that is subsequently dismutated to form H_2O_2. The main intracellular sources of H_2O_2 are the mitochondrial electron transport chain (ETC) and NADPH oxidases located in the plasma membrane, endoplasmic reticulum, and nucleus [1]. The Redox Signaling field has rapidly emerged following the discovery that endogenously formed H_2O_2 serves as a second messenger. Redox signaling proceeds through the specific and reversible oxidation of dedicated cysteines in proteins, and over the past few decades the involvement of redox signaling downstream of H_2O_2 in the regulation of a wide range of vital processes has become apparent [2–4]. Cell fate downstream of redox signaling may range from enhanced proliferation [5] and differentiation [6–8] to induction of cell death dependent on where and how much H_2O_2 is produced [9,10], reviewed in Ref. [11].

With the development of sensitive techniques to detect H_2O_2 in live

Abbreviations: DAAO, D-amino acid oxidase; OCR, Oxygen consumption rate.

* Corresponding author.
E-mail address: T.B.Dansen@umcutrecht.nl (T.B. Dansen).
[1] present address: Hubrecht Institute, Uppsalalaan 8,3584 CT Utrecht, The Netherlands.
[2] These authors contributed equally.

https://doi.org/10.1016/j.freeradbiomed.2023.06.030
Received 15 May 2023; Received in revised form 18 June 2023; Accepted 26 June 2023
Available online 29 June 2023

cells [12–15], it became clear that endogenous H_2O_2 is characterized by steep concentration gradients, and hence does not diffuse far from its site of production [4,7,14,16–18]. These observations also strengthened the notion that redox signaling should preferably be studied under conditions that best mimic physiological circumstances [19]. Hence, using localized, low levels of steady state H_2O_2 production rather than bolus addition of exogenous H_2O_2. To this end, the redox biology field has embraced a chemogenetic approach to achieve inducible, titratable, and targetable endogenous H_2O_2 production that makes use of the ectopic expression of the enzyme D-amino acid oxidase (DAAO, E.C. 1.4.3.3) from the yeast *R. gracilis* [20–22]. Administration of D-amino acids, which are normally (largely) absent from culture media and animal model systems, is subsequently used to induce H_2O_2 production (Fig. 1). The DAAO system has been used recently in a variety of studies aimed at e.g., measuring whether H_2O_2 produced in the mitochondrial matrix is released to the cytosol or to study the isolated effect of oxidative damage in the hearts of rats in the absence of other cardiac pathology. A (non-exhaustive) overview of recent studies applying *R.gracilis* DAAO to generate H_2O_2 *in vivo* or in live cells is provided in Table 1.

Many of these studies make use of fluorescence-based H_2O_2 sensors like HyPer7 as a means to quantify H_2O_2 production by DAAO. These sensors can be either expressed as a fusion protein of DAAO or expressed separately, for instance with a different localization tag to assess H_2O_2 gradients across organelles [22–24]. This approach can report on relative H_2O_2 levels within one model system, but it may not be suitable to directly compare DAAO activity, and therefore H_2O_2 levels under varying conditions or when DAAO is expressed at different subcellular sites. DAAO activity is dependent on its expression level, localization, presence of the cofactor FAD and availability of its substrate D-amino acids. The latter will likely not only depend on how much substrate has been administered to the culture media, but also on its uptake, and diffusion and transport rates across organellar membranes. Furthermore, genetically encoded fluorescent sensors like HyPer7 report on the *combined* rates of oxidation (by H_2O_2) and reduction (by the thioredoxin system in case of HyPer7) [25], and therefore its ratiometric readout depends not only on DAAO activity but also on the local reductive capacity, which varies between organelles and cell lines [26]. Hence, absolute levels of H_2O_2 produced by DAAO and H_2O_2 concentration measured with for instance HyPer7 may not necessarily be directly proportional, and this may influence conclusions drawn. Besides, HyPer7 itself could in principle affect the reductive capacity by acting as an H_2O_2 sink, making comparisons between conditions and cell lines even more difficult.

We have developed an assay that reports directly on DAAO activity independent of the local reductive capacity. Since H_2O_2 production by DAAO consumes an equimolar amount of oxygen, DAAO activity can be determined by measuring the oxygen consumption of cells upon the addition of D-amino acids using for instance a Seahorse XFe Analyzer, which is a widely available piece of equipment in research institutes. We show that this method can be used to quantify DAAO activity in monoclonal RPE1-hTERT cell lines that express the enzyme at various

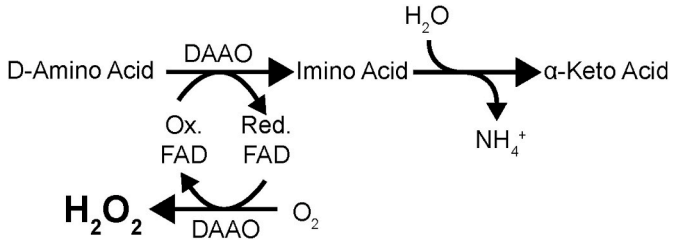

Fig. 1. Schematic of the reaction catalyzed by DAAO.
DAAO converts D-amino acids to imino acids, reducing its cofactor FAD. FAD is subsequently oxidized, generating H_2O_2 while consuming equimolar amounts of O_2. The formed imino acids spontaneously hydrolyze to α-keto acids.

Table 1
A selection of recent studies using ectopic expression of *R. gracilis* DAAO.

Study topic	Localization & References
Role of H_2O_2 in neuronal health and development	Expression of DAAO without localization sequence [21] Expression of membrane-associated DAAO [27]
DAAO as putative anti-cancer therapy	*In vivo* injection of recombinant DAAO [28] Addition of recombinant DAAO to cells [29] Expression of DAAO without localization sequence [20,30]
Mitochondrial H_2O_2 dynamics and release	Expression of mitochondrial matrix, peroxisomal and ER DAAO [31] Expression of mitochondrial matrix and cytosolic DAAO [32] Expression of mitochondrial matrix DAAO [14,33]
Oxidative heart failure in rats and mice	Expression of nuclear DAAO in cardiomyocytes *in vivo* [34] Expression of cytosolic DAAO in cardiomyocytes *in vivo* [35–37]
ROS-dependent cell cycle regulation	Expression of nuclear and cytosolic DAAO [5]
Nuclear redox environment	Expression of nuclear DAAO [38] [a]

[a] This study uses human DAAO.

subcellular sites. This allowed us to determine and directly compare at what levels H_2O_2 impairs viability when produced in different compartments. We show that intramitochondrial H_2O_2 production prevents outgrowth of cells at much lower levels as compared to production at the outer mitochondrial membrane or near the genomic DNA. We also provide evidence that the uptake of D-amino acids competes with that of L-amino acids and that D-amino acid uptake is a rate-limiting step in intracellular DAAO-dependent H_2O_2 production. We think that our OCR-based approach to directly quantify H_2O_2 production levels is of value to the redox biology community and could be applied to the quantification of other enzyme activities that consume or produce oxygen as a byproduct.

2. Results

2.1. Oxygen consumption rate can be used as a proxy for DAAO activity

We hypothesized that if the activity of ectopically expressed DAAO would be high enough as compared to other oxygen dependent cellular reactions, DAAO activity could be directly monitored by measuring the oxygen consumption rate (OCR) in a Seahorse XFe24 analyzer. The standard injection ports of the machine can be used for the addition of D-amino acids, allowing for baseline and induced OCR measurements within the same run. We used D-Ala (CID 71080) with the rationale that its other reaction products besides H_2O_2 (i.e. pyruvate and ammonia) are abundantly present and rapidly metabolized, and therefore relatively minor increases in the flux of these metabolites would have negligible effects on cell physiology or OCR. Most previous studies using DAAO also used D-Ala as a substrate. To minimize variation, in this study we used monoclonal Human RPE1-hTERT cells that stably expressed *R. gracilis* DAAO (without its C-terminal peroxisomal localization signal SKL) fused to various localization tags as well as mScarlet. Localization tags used in this study can be found in Table 2.

Fig. 2A shows that an increase in OCR upon addition of D-Ala (using L-Ala (CID 5950) as a control) can indeed be observed in RPE1-hTERT-$^{TOM20-DAAO}$ cells. At 20 mM D-Ala, the H_2O_2 production is about 60 pmol/min which translates to ~1.5 fmol cell^{-1} min^{-1}. OCR before addition of D-Ala consists predominantly of mitochondrial respiration as this can be largely inhibited by the ATP synthase inhibitor oligomycin (CID 52947716) (Fig. 1A). Metabolic differences between wells are expected to be largely eliminated by addition of Oligomycin, yielding a more reliable baseline that correlates better with cell number.

Table 2
Utilized localization tags to target DAAO.

abbreviation	Localization tag and targeted compartment	Model for which endogenous H_2O_2 source
TOM20	Targeting sequence of human TOMM20; cytosolic side of the outer mitochondrial membrane	Release of H_2O_2 from mitochondria
H2B	Human Histone 2B; Nucleosome	H_2O_2 production close to the genomic DNA (e.g. as done by LSD1)
MLS	2 x Presequence of human COX-8; Mitochondrial matrix	H_2O_2 production in the mitochondrial matrix.
IMS	Presequence of human DIABLO; Mitochondrial Intermembrane space	H_2O_2 production in the mitochondrial intermembrane space.

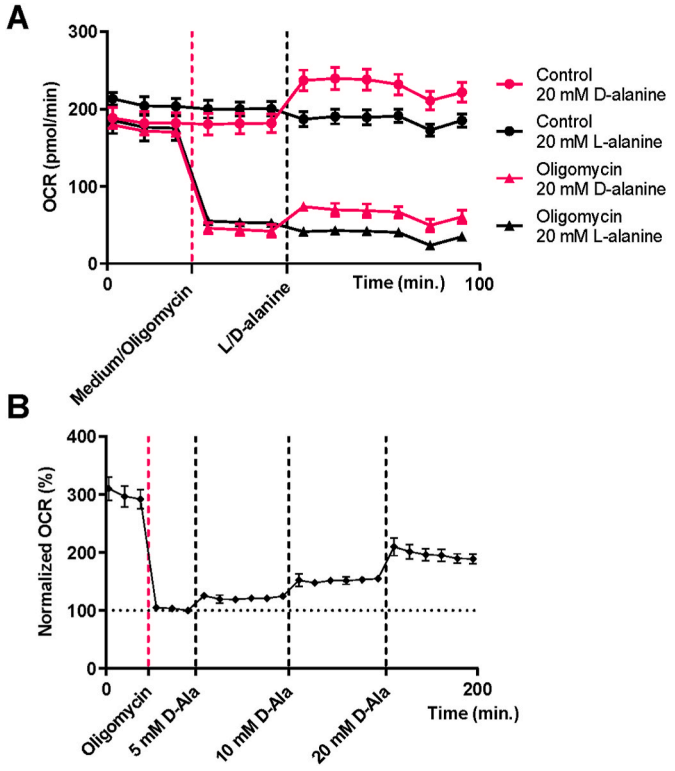

Fig. 2. H_2O_2 production by ectopically expressed DAAO can be estimated by measuring oxygen consumption in a Seahorse XF analyzer.
A. RPE1-hTERT$^{TOM20-DAAO}$ cells treated with L- or D-Ala in the presence and absence of oligomycin. Treatment with D-Ala, but not L-Ala leads to an increased OCR. Oligomycin inhibits mitochondrial respiration, resulting in more reliable estimation of DAAO-dependent OCR with lower signal-to-noise ratio. The error bars represent the standard deviation of 2–3 technical replicates (multiple wells per condition in one Seahorse plate). Typical result of several biological replicates. B. Sequential injections show [D-Ala] dependent increases in the mean OCR of RPE1-hTERT$^{TOM20-DAAO}$ cells. The third timepoint after oligomycin addition was set to 100%. Note that addition of oligomycin decreases the variability of the measurements between wells. The indicated [D-Ala] on the horizontal axis represents the total [D-Ala] in the well after each injection. Error bars: standard deviation of 5 technical replicates. Typical result of at least 4 independent experiments with similar conditions.

Furthermore, DAAO-induced OCR can in this way be compared to the OCR that stems from mitochondrial respiration, to estimate whether the observed rates are near-physiological or not. It has been estimated that under basal conditions about 1% of oxygen passing through the ETC ends up as superoxide [39,40], and two superoxide molecules will generate one molecule of H_2O_2 (catalyzed by SOD). Fig. 2B shows that oligomycin treatment indeed provides a larger relative increase above baseline, allowing for more robust measurements.

Each well in a Seahorse XF Analyzer has four injection ports. DAAO activity can thus be titrated using increasing D-amino acid concentrations in a single well. This allows for the comparison of the DAAO activity across a range of incremental D-Ala concentrations, without having to use different wells (and normalization) for each D-Ala concentration (Fig. 2B), the oligomycin-normalized oxygen consumption of RPE1-hTERT$^{TOM20-DAAO}$ cells is shown at different concentrations of D-Ala. Fig. 2B also shows that normalization to the OCR after oligomycin treatment eliminates most variation across different wells. The DAAO-dependent OCR is linearly proportional to the applied extracellular concentration of D-Ala over the tested range (0–20 mM). A plateau in OCR is observed for each concentration, suggesting that also at the lowest applied concentration substrate does not become limiting over the time-course of the measurement (50 min following each addition).

2.2. The HyPer7 signal is dependent on glucose availability

Glucose metabolism is a major source of the reducing equivalent NADPH, and HyPer7 reports on the combined rate of oxidation (by H_2O_2) and reduction (by Thioredoxin). We compared the cytosolic NES-HyPer7 signal in response to H_2O_2 produced by DAAO^{TOM20} cultured in media containing either 1 g/L or 4.5 g/L glucose. Indeed, the oxidized/reduced HyPer7 ratios in low glucose media are much higher as compared to those in high glucose media at the same concentration of D-Ala (Fig. 3). Under low glucose conditions the HyPer7 ratio increases roughly twice as fast as under high glucose conditions at [D-Ala] $\leq$ 10 mM. Above 20 mM [D-Ala] or when a bolus of exogenous H_2O_2 is provided, oxidation of the HyPer7 probe seems to outcompete reduction also under high glucose conditions. This example illustrates that HyPer7 indeed reports on H_2O_2 dependent changes in the ratio of oxidation and reduction and not directly on H_2O_2 levels, and that care should be taken to keep culture conditions identical when HyPer7 is used to estimate or compare H_2O_2 levels. Because the rate of H_2O_2 production can be deduced from the OCR experiments, the relative reductive capacity of the cytosol under different conditions can be estimated from the HyPer7 ratio.

2.3. Transmembrane transport of D-amino acids can be a rate limiting factor for DAAO activity and depends on the specific D-amino acid used

Based on the reported *in vitro* Michaelis-Menten constant for DAAO using D-Ala as a substrate (2.6 mM) [41], one would expect that DAAO activity would be ~75% saturated at 5 mM and almost 95% saturated at 10 mM of D-Ala. Our experiments in live cells however suggest a linear increase in DAAO activity upon an extra addition of 10 mM D-Ala (to yield a total of 20 mM) and hence an apparent K_M that is much higher than 2.6 mM. To test whether the rate of import of D-Ala over the plasma membrane could be a limiting factor for DAAO activity we permeabilized 20 mM D-Ala treated RPE1-hTERT$^{TOM20-DAAO}$ cells in the Seahorse machine by adding Saponin (CID 198016) or Digitonin (CID 6474107) from the third injection port. Indeed, permeabilization leads to a rapid increase in DAAO-dependent OCR (Fig. 4A). D-Ala likely uses the same amino acid importer as L-Ala, and several other amino acids [42]. Indeed, an injection with an excess of L-Ala subsequently decreased the D-Ala induced OCR, suggesting that L-Ala and D-Ala compete for the same import machinery (Fig. 4B). This observation is in line with a previous study by Erdogan et al., which demonstrated that the presence of L-Ala in the media results in decreased HyPer7 oxidation when D-Ala was administered to DAAO-expressing cells [23].

It has been observed that the rate and extent of HyPer7 oxidation upon DAAO activation is dependent on the type of D-amino acid used [23]. For instance, D-Phe (CID 71567) addition was shown to result in a faster plateau in HyPer7 oxidation levels as compared to D-Ala. To investigate whether we could corroborate these findings with our method, we compared OCR upon addition of different concentrations of

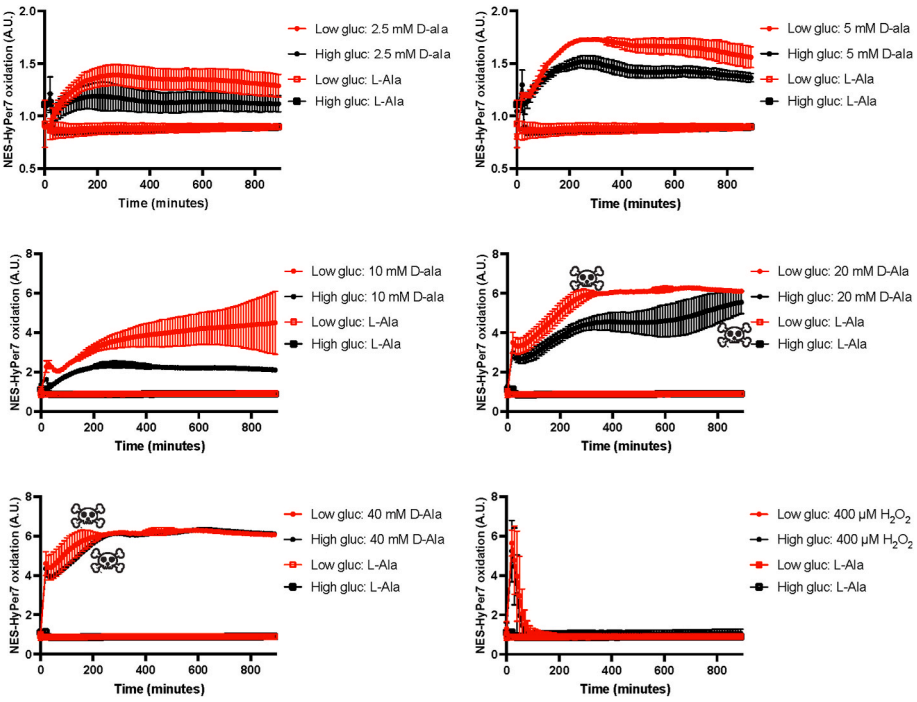

Fig. 3. HyPer7 is not solely dependent on DAAO-activity but also on glucose availability.
Measurements of NES-HyPer7 oxidation in RPE1-hTERT-DAAO^{TOM20} cells cultured in either low glucose (1 g/L) or high glucose (4.5 g/l) conditions. The skull symbols indicate the induction of massive cell death as judged by cellular morphology. Upon activation of DAAO, HyPer7 oxidation increases more rapidly and to a higher level in low glucose media compared to high glucose media. Only at very high oxidative insults (>20 mM D-Ala or 400 µM of exogenous H_2O_2) a similar oxidation of HyPer7 is detected irrespective of media glucose concentration. This illustrates that assessment of DAAO-dependent H_2O_2 production using HyPer7 measurements can be influenced by factors like glucose availability. The graphs show changes over time of the mean values and standard deviation of the mean HyPer7 ratios of >250 cells in view in two biological replicates (HyPer7 ratio was set to 1 at t = 0, before addition of D-Ala).

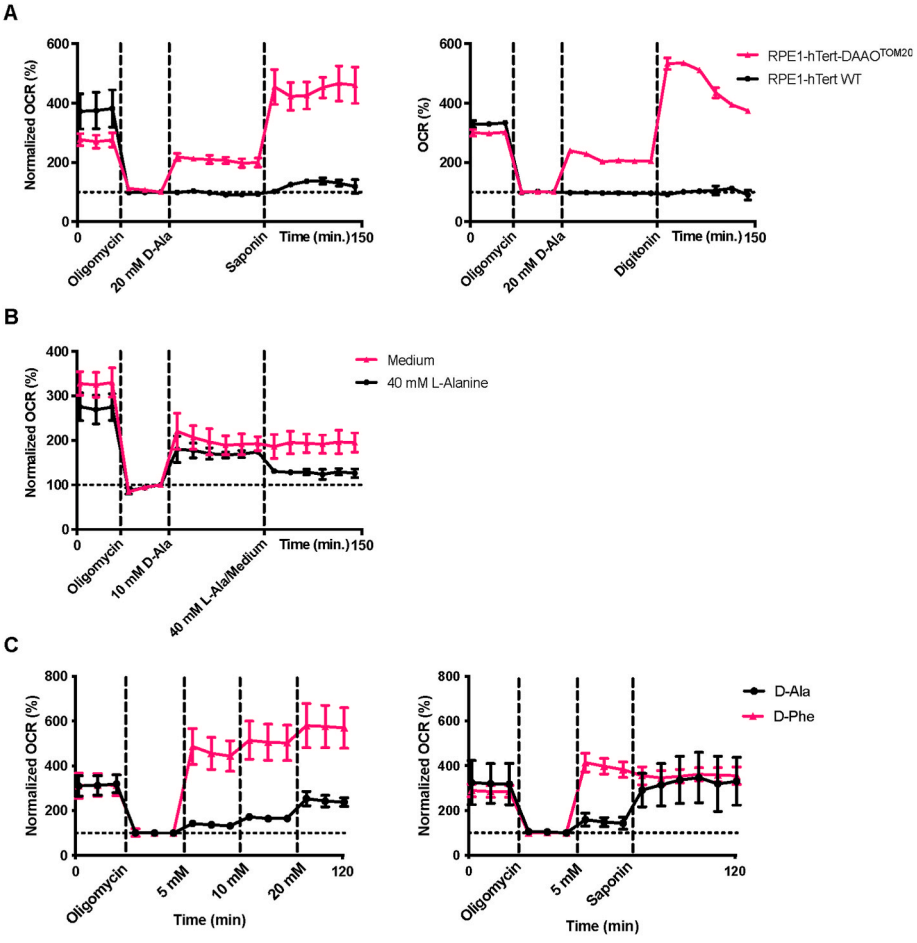

Fig. 4. Transmembrane transport of D-Ala is a rate limiting factor for DAAO activity.
A. Normalized OCR of RPE1-hTERT$^{TOM20-DAAO}$ and parental RPE1-hTERT cells treated with oligomycin, 20 mM D-Ala and 25 µg/mL saponin or digitonin at the indicated intervals. These concentrations of saponin and digitonin lead to permeabilization of the cell membrane [43]. Permeabilization leads to a rapid ~ two-fold increase in DAAO activity, indicating that transmembrane transport of D-alanine is a rate limiting factor in DAAO activity. The third timepoint after oligomycin addition was set to 100%. The error bars represent the standard deviation of 2 technical replicates. One example out of two independent experiments with similar conditions is shown. B. Normalized OCR of RPE1-hTERT-$^{TOM20-DAAO}$ cells treated with oligomycin, 10 mM D-alanine and 40 mM L-Ala (media as control). The addition of a surplus of L-Ala decreases DAAO activity, suggesting L-Ala competes with D-Ala for transport over the membrane. The third timepoint after oligomycin addition was set to 100%. The error bars represent the standard deviation of 2 technical replicates. C. Normalized OCR of RPE1-hTERT-$^{TOM20-DAAO}$ cells treated with oligomycin and different concentrations of D-Ala and D-Phe (left), or one concentration followed by subsequent saponin injection (right). D-Phe addition leads to higher levels of OCR as compared to D-Ala, and differences between D-Phe and D-Ala disappear upon permeabilization of the plasma membrane, suggesting that the higher DAAO activity upon D-Phe addition is due to a higher rate of transport over the plasma membrane. The third timepoint after oligomycin addition was set to 100%. The error bars represent the standard deviation of 8–10 technical replicates (separate wells of cells measured within the same experiment).

D-Ala and D-Phe (Fig. 4C left). Indeed, addition of 5 mM of D-Phe led to a substantial higher OCR as compared to D-Ala. In contrast to D-Ala, further increasing the concentration of D-Phe led only to a minor relative OCR increase, indicating that the intracellular [D-Phe] already surpassed the Michaelis-Menten constant for DAAO at 5 mM D-Phe in the extracellular environment. The difference in apparent enzyme kinetics between D-Ala and D-Phe was no longer observed upon membrane permeabilization by saponin injection (Fig. 4C right), demonstrating that the enhanced concentration-dependent increase in OCR upon D-Phe injection is facilitated by faster uptake. Unlike observed for D-Ala, membrane permeabilization by saponin injection did not further enhance the OCR when D-Phe was used as a substrate, suggesting that transmembrane transport of D-Phe is not rate limiting for DAAO activity.

2.4. OCR analysis enables the calibration of cell lines expressing DAAO in different compartments

We next used our Seahorse technology-based assay to calibrate and select monoclonal RPE1-hTERT cell lines that have similar DAAO activity, but that express DAAO at different subcellular locations. These cell lines could help to elucidate whether an H_2O_2-induced phenotype is indeed the result of differential localized production or due to a difference in DAAO activity and ensuing overall oxidative burden. To this end, we lentivirally transduced RPE1-hTERT cells with constructs expressing DAAO fused to various localization tags (See Table 2) and generated monoclonal lines. Fig. 5B shows that different monoclonal lines expressing DAAO targeted to the same location can indeed can have different DAAO activities.

Clones with similar DAAO activities were selected based on OCR measurements using increasing [D-Ala]. RPE1-hTERT-DAAO^{IMS} clone 2

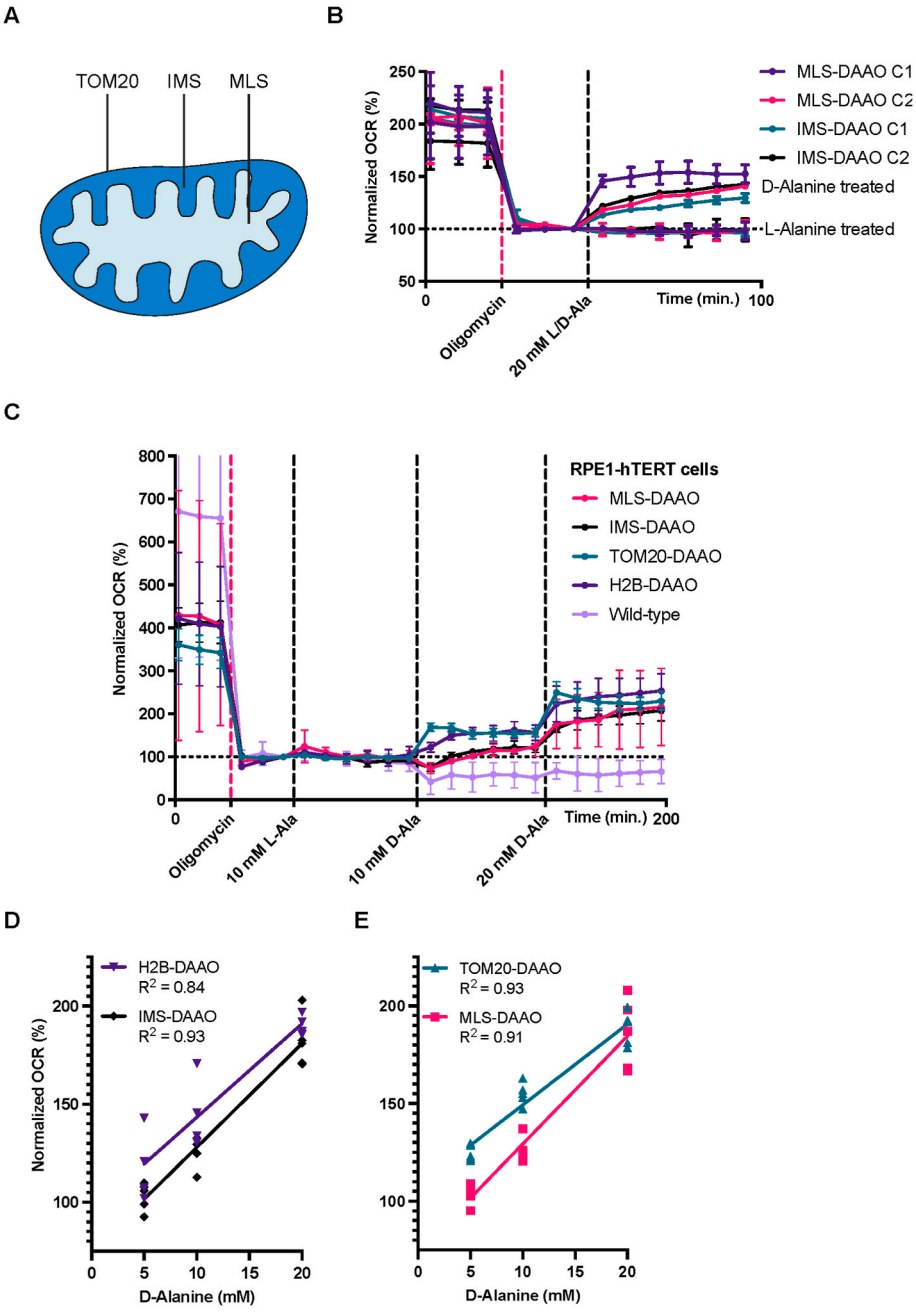

Fig. 5. RPE1-hTERT- MLS-, IMS-, TOM20-and H2B-DAAO cells produce comparable levels of H_2O_2.
A. Schematic overview of the localization of TOM20-, IMS- and MLS-DAAO constructs. H2B-DAAO is localized to nucleosomes (not shown). B. Normalized OCR of different MLS- and IMS-DAAO clones. MLS-DAAO clone 2 and IMS-DAAO clone 2 cells have a very similar level of oxygen consumption/DAAO activity at 20 mM D-Ala. The third timepoint after oligomycin addition was set to 100%. The error bars represent the standard deviation of 2–3 technical replicates. C. Normalized OCR of MLS-, IMS-, TOM20-and H2B-DAAO cells treated with sequential injections of D-alanine. D-alanine treatment of MLS-, IMS-, TOM20- and H2B-DAAO cells leads to comparable levels of DAAO activity. Wild-type cells and L-Ala-treated cells do not show increased oxygen consumption. The third timepoint after oligomycin addition was set to 100%. The indicated D-Ala concentrations represent the total concentration of D-Ala in the well after each injection. The error bars represent the standard deviation of 4 technical replicates. One example of two independent experiments with similar conditions is shown. D. Normalized OCR of DAAO cells plotted against the D-Ala concentration. DAAO activity seems to increase proportionally with the D-Ala concentration. The third timepoint after oligomycin addition was set to 100%. Each dot represents a technical replicate. TOM20-DAAO data is also displayed in Fig. 2B. The trendlines were calculated using simple linear regression. Similar results were obtained in multiple replicates with similar conditions.

and RPE1-hTERT-DAAO^{MLS} clone 2 had very similar levels of DAAO activity (Fig. 5B), and so did the RPE1-hTERT-DAAO^{H2B} and RPE1-hTERT-DAAO^{TOM20} clones but note that the activity of the MLS and IMS localized DAAO was lower as compared to H2B and TOM20 localized DAAO (Fig. 5C–D), and we did not find clones with equal activity at all four localizations. The RPE1-hTERT-DAAO^{H2B} and RPE1-hTERT-DAAO^{TOM20} cells consumed an amount of oxygen equivalent to roughly 20% of the basal mitochondrial respiration at 10 mM D-alanine. For MLS- and IMS-DAAO cells, this was 7%. These numbers are much higher than what can likely be achieved physiologically. Lowering [D-Ala] further will result in (near) physiological H_2O_2 levels, but these would be more difficult to pick up in this assay. The lower DAAO activity in the RPE1-hTERT-DAAO^{IMS} and RPE1-hTERT-DAAO^{MLS} lines should be considered when comparing the effects of DAAO-derived H_2O_2. Using a range of [D-Ala] in experiments could help to achieve similar rates of H_2O_2 production in all four lines.

2.5. The site of H_2O_2 production determines its lethal dose

An advantage of using these OCR-based calibrated monoclonal RPE1-hTERT-DAAO cell lines is the possibility to directly compare phenotypes downstream of equal but differentially localized H_2O_2 production. This may uncover for instance differences in local reductive capacity or the engagement of different signaling cascades. As an example, we have used the four monoclonal RPE1-hTERT-DAAO cell lines to measure whether changes in cell viability in response to localized H_2O_2 production depend on the site of production. Cell viability was also somewhat decreased at higher levels of the L-Ala control in all four lines, which could be due to competition with essential amino acids for the same transporter. This observation suggests that care should be taken when studying the effects of redox signaling on cell cycle using the DAAO system, and that ideally equimolar amounts of L-Ala should be used as a control for D-Ala. Production of H_2O_2 at the nucleosome or the cytosolic side of the outer mitochondrial membrane shows a sudden decrease in cell viability at ~20 mM D-Ala, whereas H_2O_2 production in the mitochondrial intermembrane space or matrix showed a more gradual drop in viability, starting already at 2.5 mM D-Ala (Fig. 6 & Sup. Fig. 1). Note that the DAAO activity in the RPE1-hTERT-DAAO^{MLS} and RPE1-hTERT-DAAO^{IMS} was about half that of DAAO activity in RPE1-hTERT-DAAO^{H2B} and RPE1-hTERT-DAAO^{TOM20} cells at equal [D-Ala], which makes the difference in response even bigger.

3. Discussion

The use of yeast D-amino acid oxidase has recently spurred research on intercompartmental H_2O_2 diffusion and signaling. However, as far as we know an assay that reports on the DAAO activity in live cells independently of the local reductive capacity has not been described before. The here described OCR-based DAAO activity assay can be used to compare DAAO activity across different cell lines, subcellular compartments, and D-alanine concentrations and gradients, irrespective of differences in local or global reductive capacity. This allows the establishment of DAAO model systems with comparable levels of H_2O_2 production, to distinguish phenotypic effects that stem from differences in for instance reductive capacity or total oxidative burden. By combining this assay with ultrasensitive, genetically encoded H_2O_2 sensors like roGFP2-Tsa2 and Hyper7, the (local) reductive capacity could be estimated by comparing the DAAO-dependent OCR with the Hyper7 signal, although it should be noted that these two parameters can as yet not be assessed simultaneously within the same well of cells.

The use of oligomycin in the assay makes it possible to compare DAAO-dependent H_2O_2 production to the amount of oxygen used in mitochondrial respiration. Mitochondrial respiration is a major source of ROS but the estimates of what percentage of oxygen used in mitochondrial respiration 'escapes' as superoxide and subsequently forms H_2O_2 are quite variable in literature. Often a value of 1–2% is reported

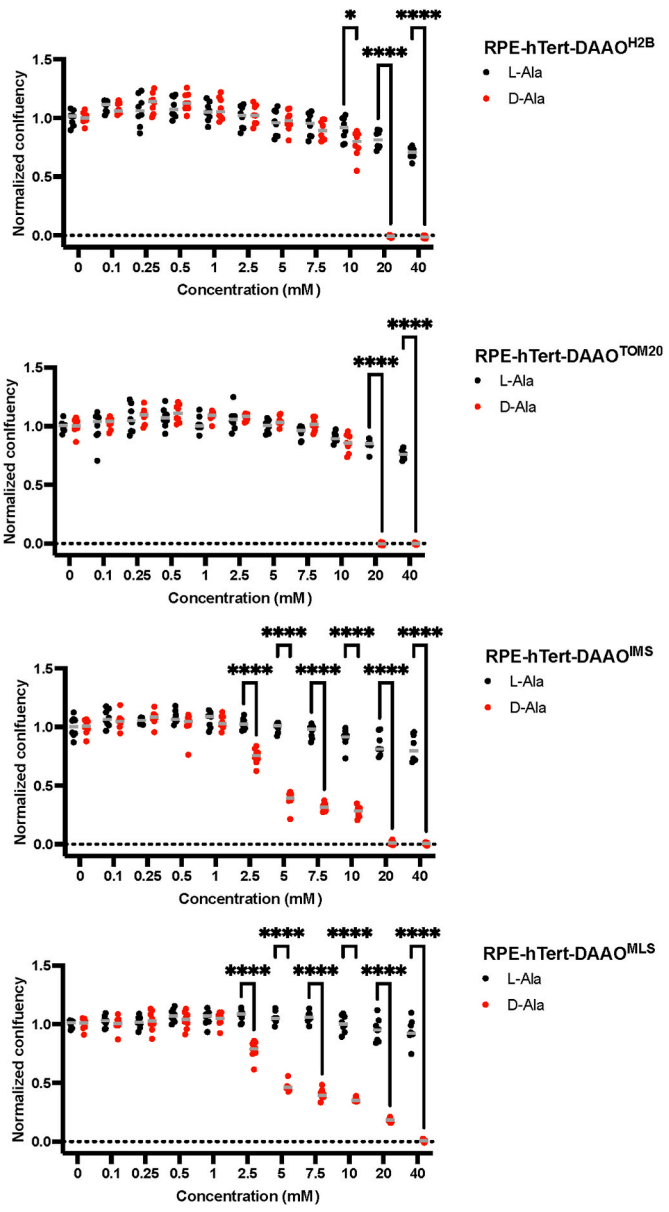

Fig. 6. The subcellular site of H_2O_2 production determines its lethal dose
Quantification of crystal violet assay shown in sup. Fig. 1 with RPE-1-hTERT-DAAO lines treated with increasing concentrations of L- or D-Ala for 48h. The decrease in confluency is not only dependent on the D-Ala concentration used, but also on the subcellular location of DAAO. Statistical significance was determined by 2-way Anova + Šídák's multiple comparisons test (* = $p < 0.05$, **** = $p < 0.0001$, n = 8). A typical result of at least 3 replicate experiments with similar setup is shown.

based on pioneering work with isolated mitochondria [39,44]. More recently, however, far lower estimations between 0.1% and 0.5% have been reported [45–48]. Brand [48] even suggests that mitochondrial H_2O_2 generation is not directly related to the amount of mitochondrial respiration. It is therefore difficult to make a good estimate of what DAAO-dependent OCR is comparable to physiological levels of (mitochondrial) H_2O_2 production. However, at the levels of DAAO expression in our cell lines a substrate concentration of 2.5 mM D-Ala yields already more H_2O_2 than the maximum estimates mentioned in literature. At 10 mM D-Ala the amount of oxygen used for DAAO-dependent H_2O_2 production was as much as 7–20% of basal mitochondrial OCR. The exact percentage depended on the monoclonal line and may therefore not be directly translated to other systems using DAAO expression. Note that

oligomycin blocks ATP synthase and thereby inhibits OCR indirectly, whereas a combination of antimycin A and rotenone could potentially decrease mitochondrial OCR even further. We do however not expect that this would lead to much more accurate comparisons of DAAO-dependent OCR to mitochondrial OCR.

The observed differences in H_2O_2 production between clones expressing the same localized DAAO protein are likely to be caused by variable expression of DAAO (Fig. 5B). However, we also observe that certain DAAO localizations tend to display lower activity compared to others; DAAO expressed within mitochondria shows substantial lower levels of H_2O_2 production compared to $DAAO^{H2B}$ and $DAAO^{TOM20}$ (Fig. 5C). While localization signals may affect protein expression and turnover, these differences might also stem from differential availability of D-alanine and/or FAD across cellular compartments. The transport of D-Ala over the plasma membrane is rate limiting (Fig. 4A), and transport over additional intracellular membranes is likely to also cause differences in [D-Ala] between subcellular compartments. The advantage of using OCR as a readout for H_2O_2 production is that DAAO activity between compartments can still be compared despite compartmental differences in for instance [D-amino acid], [FAD] or reductive capacity.

The OCR-based DAAO activity assay can in principle also be applied to other oxidases. Seahorse XF analyzers have previously been used to measure the activity of a genetically encoded NADPH oxidase, LbNOX [49]. Similarly, the activity of a genetically engineered NADPH oxidase and H_2O_2 generator, P450 BM3, might also be estimated by measuring its oxygen consumption [50]. But since these enzymes use substrates that are, unlike D-amino acids, present normally in cultured cells it is more difficult to compare baseline and induced activity for these NADPH oxidases.

There are also some points to consider regarding the OCR-based DAAO activity assay. Firstly, it is difficult to measure levels of DAAO activity that are smaller than the variations in baseline OCR, even in oligomycin-treated cells. Increased oxygen consumption could reliably be measured upon addition of 5 mM D-alanine, but the corresponding levels of H_2O_2 production are probably already supraphysiological. At lower D-alanine concentrations H_2O_2 levels must therefore be extrapolated, which comes with the risk that for some reason the mathematical relationship between [D-Ala] and [H_2O_2] changes at [D-Ala] < 5 mM. Secondly, H_2O_2 that is reduced by catalase yields molecular oxygen, and therefore this fraction of H_2O_2 no longer contributes to OCR. The DAAO-dependent OCR may therefore underestimate the amount of H_2O_2 produced. Since catalase is localized to peroxisomes this may not be a major issue.

Besides these practical concerns, it is important to keep in mind that the OCR-based DAAO activity assay measures the amount of H_2O_2 produced by DAAO and not the resulting H_2O_2 concentration. If DAAO is localized to a relatively small subcellular compartment, a higher H_2O_2 concentration may be reached compared to equal DAAO activity in a larger compartment (assuming H_2O_2 does not diffuse out of the compartment).

Despite these limitations, we think that the method described here will contribute to a better understanding of DAAO-based model systems to generate H_2O_2 and by extension move the redox biology field forward.

4. Materials

REAGENT or RESOURCE	SOURCE	IDENTIFIER
Chemicals, peptides, and recombinant proteins		
2-Deoxyglucose	Acros Organics	111980250
Blasticidin	Bio Connect	ant-bl-1
d-alanine	Sigma-Aldrich	A7377
d-Phenylalanine	Sigma-Aldrich	P1751
Digitonin	Sigma-Aldrich	D141
DMEM/F12	Sigma-Aldrich	D8062
DMEM High glucose	Sigma-Aldrich	D6429
DMEM Low glucose	Sigma-Aldrich	D5546
Fetal Bovine Serum	Bodinco	BDC-17748
Glucose	Merck Millipore	1.08337.1000
l-alanine	Sigma-Aldrich	A7627
l-glutamine	Lonza	17-605E
NaOH	Merck Millipore	1.06498.1000
Oligomycin	Sigma-Aldrich	75351
Penicillin-streptomycin	Lonza	DE17602E
Polybrene	Sigma Aldrich	TR-1003
Rat tail collagen 1	Corning	354236
Saponin	Sigma-Aldrich	47036-250G-F
Seahorse XF base media	Agilent	102353–100
Seahorse XF Calibrant	Agilent	102353–100
Sodium Pyruvate	Sigma-Aldrich	S8636
Trypsin	Sigma-Aldrich	T3924
Critical commercial assays		
Pierce™ BCA Protein assay kit	Thermo Scientific	23225
Seahorse XF24 V7 PS cell culture microplates	Agilent	100777–004
Seahorse XFe24 FluxPak	Agilent	102340–100
Experimental models: Cell lines		
RPE1-hTERT H2B-DAAO		
RPE1-hTERT IMS-DAAO		
RPE1-hTERT MLS-DAAO		
RPE1-hTERT TOM20-DAAO		
RPE1-hTERT TOM20-DAAO + NES-HyPer7		
Software and algorithms		
FIJI imaging software	https://fiji.sc/	
GraphPad Prism 9.3.1	https://www.graphpad.com/scientific-software/prism/	
Wave Desktop and Controller 2.6 Software	https://www.agilent.com/en/product/cell-analysis/real-time-cell-metabolic-analysis/xf-software/seahorse-wave-desktop-software-740897	
Other		
iMark Microplate Absorbance reader	Bio-Rad	1681130
Seahorse XFe24 analyzer	Aligent	420017
ZEISS Cell Observer microscope	ZEISS	N.A.

5.1. Cell culture & lentiviral transduction

RPE1-hTERT cells were cultured in DMEM/F-12 supplemented with 10% FBS, 2 mM L-glutamine and 100 Units Penicillin-Streptomycin. The cells were cultured at 37 °C under a 6% CO2 atmosphere. The IDT (www.idtdna.com) codon optimization tool was used to convert the DAAO cDNA sequence from *Rhodotorula gracilis* for expression in human cells. The C-terminal peroxisomal targeting sequence was removed and a geneblock (see Supplementary information) was ordered for further cloning (Integrated DNA technologies). Fusions with the H2B-, TOM20-, IMS- and MLS-DAAO signals in a pLenti backbone were made by infusion cloning. DAAO-expressing cells were generated using lentiviral infection and were subsequently made monoclonal by single-cell sorting. Generation of NES-HyPer7 lentiviruses and infection of TOM20-DAAO cells was performed as described previously [51]. After infection, TOM20-DAAO + NES-HyPer7 cells with high HyPer7 fluorescence were single-cell sorted in conditioned media and expanded to generate monoclonal cell lines.

5. Methods

5.2. Determination of OCR using a Seahorse XFe analyzer

A Seahorse Bioscience XFe24 Analyzer was used to measure of oxygen consumption rates of RPE DAAO cells. A day before the assay, 24-well V7 Seahorse culture plates were coated with 50 μL of 50 μg/mL rat tail collagen 1 in 0.1% acetic acid for 20 min at room temperature. Afterwards the plate was washed with PBS and 40,000 cells were seeded in 100 μL media. To 4 wells 100 μL of media containing no cells was added to serve as background correction. After the cells had attached, an additional 150 μL of media was added. In parallel, the Seahorse sensor cartridge was hydrated with Seahorse calibrant solution a day before the assay. Similarly, the Seahorse XFe24 analyzer was also turned on at this time to let it warm up overnight. On the day of the assay, cells were washed twice with assay media (XF base media supplemented with 2 mM L-glutamine, 17.5 mM glucose, 1 mM Sodium Pyruvate and 0.5 mM NaOH). Cells were incubated for 60 min in assay media in a non-CO_2, humidified incubator at 37 °C before starting the assay. Injections of L/D-alanine, 2 μM oligomycin, 25 μg/mL saponin and digitonin were used. The oxygen consumption rate was normalized to the oxygen consumption rate measured 25 min after oligomycin injection. For more details on the Seahorse-based DAAO activity assay see addendum 1.

5.3. HyPer7 live imaging

For measuring HyPer7 oxidation by live microscopy, we refer to the method described previously by our laboratory [52].

5.4. Crystal violet-based viability and outgrowth assay

Cells were counted after trypsinization and seeded in 96-well plates at a density of $0.5 \bullet 10^4$ cells per well. The next day, cells were exposed to a concentration range of [D-Ala] using the same concentrations of L-Ala as a control. D/L-Ala was left on the cells for 48 h. The plates contained 8 replicates for each cell line with a different DAAO localization and D/L-Ala concentration. Plates were washed twice with PBS, followed by fixation with ice-cold MeOH for 10 min. MeOH was aspirated and wells were overlaid with 0.5% w/v Crystal Violet in 25% MeOH for 10 min, followed by thorough washing with H_2O. 8 empty wells per 96 well plate were used as blanks. Plates were air-dried overnight and scanned on an EPSON flatbed photo scanner. Crystal Violet was redissolved by adding 100 μL of 10% Acetic Acid per well and quantified by spectrophotometry (595 nm) using a Biorad iMark plate reader.

Funding

This work was funded by a grant from the Dutch Cancer Society (KWF Kankerbestrijding) to TBD. BMTB is a member of the Oncode Institute, which is partly funded by the Dutch Cancer Society (KWF Kankerbestrijding).

Declaration of competing interest

The authors declare that they have no known competing financial interests or personal relationships that could have appeared to influence the work reported in this paper.

Acknowledgements

We would like to thank Jan Riemer and Carsten Berndt for valuable discussions, and our colleagues at the Center for Molecular Medicine, UMC Utrecht for their input and suggestions.

Appendix A. Supplementary data

Supplementary data to this article can be found online at https://doi.org/10.1016/j.freeradbiomed.2023.06.030.

References

[1] H.S. Wong, B. Benoit, M.D. Brand, Mitochondrial and cytosolic sources of hydrogen peroxide in resting C2C12 myoblasts, Free Radic. Biol. Med. 130 (2019) 140–150.
[2] K.M. Holmstrom, T. Finkel, Cellular mechanisms and physiological consequences of redox-dependent signalling, Nat. Rev. Mol. Cell Biol. 15 (6) (2014) 411–421.
[3] H. Sies, D.P. Jones, Reactive oxygen species (ROS) as pleiotropic physiological signalling agents, Nat. Rev. Mol. Cell Biol. 21 (7) (2020) 363–383.
[4] C.C. Winterbourn, Biological production, detection, and fate of hydrogen peroxide, Antioxidants Redox Signal. 29 (6) (2018) 541–551.
[5] D.G. Kirova, K. Judasova, J. Vorhauser, T. Zerjatke, J.K. Leung, I. Glauche, J. Mansfeld, A ROS-dependent mechanism promotes CDK2 phosphorylation to drive progression through S phase, Dev. Cell 57 (14) (2022) 1712–1727 e9.
[6] A. Sato, M. Okada, K. Shibuya, E. Watanabe, S. Seino, Y. Narita, S. Shibui, T. Kayama, C. Kitanaka, Pivotal role for ROS activation of p38 MAPK in the control of differentiation and tumor-initiating capacity of glioma-initiating cells, Stem Cell Res. 12 (1) (2014) 119–131.
[7] S. De Henau, M. Pages-Gallego, W.J. Pannekoek, T.B. Dansen, Mitochondria-derived H(2)O(2) promotes symmetry breaking of the C. elegans zygote, Dev. Cell 53 (3) (2020) 263–271 e6.
[8] T. Schader, O. Lowe, C. Reschke, P. Malacarne, F. Hahner, N. Muller, A. Gajos-Draus, J. Backs, K. Schroder, Oxidation of HDAC4 by Nox4-derived H(2)O(2) maintains tube formation by endothelial cells, Redox Biol. 36 (2020), 101669.
[9] L. Bleier, I. Wittig, H. Heide, M. Steger, U. Brandt, S. Drose, Generator-specific targets of mitochondrial reactive oxygen species, Free Radic. Biol. Med. 78 (2015) 1–10.
[10] E.C. Cheung, P. Lee, F. Ceteci, C. Nixon, K. Blyth, O.J. Sansom, K.H. Vousden, Opposing effects of TIGAR- and RAC1-derived ROS on Wnt-driven proliferation in the mouse intestine, Genes Dev. 30 (1) (2016) 52–63.
[11] H. Sies, V.V. Belousov, N.S. Chandel, M.J. Davies, D.P. Jones, G.E. Mann, M. P. Murphy, M. Yamamoto, C. Winterbourn, Defining roles of specific reactive oxygen species (ROS) in cell biology and physiology, Nat. Rev. Mol. Cell Biol. 23 (7) (2022) 499–515.
[12] D.S. Bilan, V.V. Belousov, In vivo imaging of hydrogen peroxide with HyPer probes, Antioxidants Redox Signal. 29 (6) (2018) 569–584.
[13] B. Morgan, K. Van Laer, T.N. Owusu, D. Ezerina, D. Pastor-Flores, P.S. Amponsah, A. Tursch, T.P. Dick, Real-time monitoring of basal H2O2 levels with peroxiredoxin-based probes, Nat. Chem. Biol. 12 (6) (2016) 437–443.
[14] V.V. Pak, D. Ezerina, O.G. Lyublinskaya, B. Pedre, P.A. Tyurin-Kuzmin, N. M. Mishina, M. Thauvin, D. Young, K. Wahni, S.A. Martinez Gache, A. D. Demidovich, Y.G. Ermakova, Y.D. Maslova, A.G. Shokhina, E. Eroglu, D.S. Bilan, I. Bogeski, T. Michel, S. Vriz, J. Messens, V.V. Belousov, Ultrasensitive genetically encoded indicator for hydrogen peroxide identifies roles for the oxidant in cell migration and mitochondrial function, Cell Metabol. 31 (3) (2020) 642–653 e6.
[15] M. Schwarzlander, T.P. Dick, A.J. Meyer, B. Morgan, Dissecting redox biology using fluorescent protein sensors, Antioxidants Redox Signal. 24 (13) (2016) 680–712.
[16] Y.G. Ermakova, N.M. Mishina, C. Schultz, V.V. Belousov, Visualization of intracellular hydrogen peroxide with the genetically encoded fluorescent probe HyPer in NIH-3T3 cells, Methods Mol. Biol. (2019) 259–274, 1982.
[17] M.N. Hoehne, L. Jacobs, K.J. Lapacz, G. Calabrese, L.M. Murschall, T. Marker, H. Kaul, A. Trifunovic, B. Morgan, M. Fricker, V.V. Belousov, J. Riemer, Spatial and temporal control of mitochondrial H(2) O(2) release in intact human cells, EMBO J. 41 (7) (2022), e109169.
[18] N.M. Mishina, Y.A. Bogdanova, Y.G. Ermakova, A.S. Panova, D.A. Kotova, D. S. Bilan, B. Steinhorn, E.S.J. Arner, T. Michel, V.V. Belousov, Which antioxidant system shapes intracellular H(2)O(2) gradients? Antioxidants Redox Signal. 31 (9) (2019) 664–670.
[19] M.P. Murphy, H. Bayir, V. Belousov, C.J. Chang, K.J.A. Davies, M.J. Davies, T. P. Dick, T. Finkel, H.J. Forman, Y. Janssen-Heininger, D. Gems, V.E. Kagan, B. Kalyanaraman, N.G. Larsson, G.L. Milne, T. Nystrom, H.E. Poulsen, R. Radi, H. Van Remmen, P.T. Schumacker, P.J. Thornalley, S. Toyokuni, C.C. Winterbourn, H. Yin, B. Halliwell, Guidelines for measuring reactive oxygen species and oxidative damage in cells and in vivo, Nat Metab 4 (6) (2022) 651–662.
[20] L.D. Stegman, H. Zheng, E.R. Neal, O. Ben-Yoseph, L. Pollegioni, M.S. Pilone, B. D. Ross, Induction of cytotoxic oxidative stress by D-alanine in brain tumor cells expressing Rhodotorula gracilis D-amino acid oxidase: a cancer gene therapy strategy, Hum. Gene Ther. 9 (2) (1998) 185–193.
[21] R.E. Haskew-Layton, J.B. Payappilly, N.A. Smirnova, T.C. Ma, K.K. Chan, T. H. Murphy, H. Guo, B. Langley, R. Sultana, D.A. Butterfield, S. Santagata, M. J. Alldred, I.G. Gazaryan, G.W. Bell, S.D. Ginsberg, R.R. Ratan, Controlled enzymatic production of astrocytic hydrogen peroxide protects neurons from oxidative stress via an Nrf2-independent pathway, Proc. Natl. Acad. Sci. U. S. A. 107 (40) (2010) 17385–17390.
[22] M.E. Matlashov, V.V. Belousov, G. Enikolopov, How much H(2)O(2) is produced by recombinant D-amino acid oxidase in mammalian cells? Antioxidants Redox Signal. 20 (7) (2014) 1039–1044.
[23] Y.C. Erdogan, H.Y. Altun, M. Secilmis, B.N. Ata, G. Sevimli, Z. Cokluk, A.G. Zaki, S. Sezen, T. Akgul Caglar, I. Sevgen, B. Steinhorn, H. Ai, G. Ozturk, V.V. Belousov,

T. Michel, E. Eroglu, Complexities of the chemogenetic toolkit: differential mDAAO activation by d-amino substrates and subcellular targeting, Free Radic. Biol. Med. 177 (2021) 132–142.
[24] S.S. Saeedi Saravi, E. Eroglu, M. Waldeck-Weiermair, A. Sorrentino, B. Steinhorn, V. Belousov, T. Michel, Differential endothelial signaling responses elicited by chemogenetic H(2)O(2) synthesis, Redox Biol. 36 (2020), 101605.
[25] P. Kritsiligkou, T.K. Shen, T.P. Dick, A comparison of Prx- and OxyR-based H(2)O(2) probes expressed in S. cerevisiae, J. Biol. Chem. 297 (1) (2021), 100866.
[26] H. Sies, Oxidative eustress: on constant alert for redox homeostasis, Redox Biol. 41 (2021), 101867.
[27] I. Amblard, M. Thauvin, C. Rampon, I. Queguiner, V.V. Pak, V. Belousov, A. Prochiantz, M. Volovitch, A. Joliot, S. Vriz, H(2)O(2) and Engrailed 2 paracrine activity synergize to shape the zebrafish optic tectum, Commun. Biol. 3 (1) (2020) 536.
[28] J. Fang, T. Sawa, T. Akaike, H. Maeda, Tumor-targeted delivery of polyethylene glycol-conjugated D-amino acid oxidase for antitumor therapy via enzymatic generation of hydrogen peroxide, Cancer Res. 62 (11) (2002) 3138–3143.
[29] M. Fuentes-Baile, D. Bello-Gil, E. Perez-Valenciano, J.M. Sanz, P. Garcia-Morales, B. Maestro, M.P. Ventero, C. Alenda, V.M. Barbera, M. Saceda, CLytA-DAAO, free and immobilized in magnetic nanoparticles, induces cell death in human cancer cells, Biomolecules 10 (2) (2020).
[30] J. Li, Y. Shen, A. Liu, X. Wang, C. Zhao, Transfection of the DAAO gene and subsequent induction of cytotoxic oxidative stress by D-alanine in 9L cells, Oncol. Rep. 20 (2) (2008) 341–346.
[31] C. Kruger, M. Waldeck-Weiermair, J. Kaynert, T. Pokrant, Y. Komaragiri, O. Otto, T. Michel, M. Elsner, AQP8 is a crucial H(2)O(2) transporter in insulin-producing RINm5F cells, Redox Biol. 43 (2021), 101962.
[32] S.J. Moon, W. Dong, G.N. Stephanopoulos, H.D. Sikes, Oxidative pentose phosphate pathway and glucose anaplerosis support maintenance of mitochondrial NADPH pool under mitochondrial oxidative stress, Bioeng. Transl. Med. 5 (3) (2020), e10184.
[33] K.T. Stein, S.J. Moon, A.N. Nguyen, H.D. Sikes, Kinetic modeling of H2O2 dynamics in the mitochondria of HeLa cells, PLoS Comput. Biol. 16 (9) (2020), e1008202.
[34] M.S. Nanadikar, A.M. Vergel Leon, J. Guo, G.J. van Belle, A. Jatho, E.S. Philip, A. F. Brandner, R.A. Bockmann, R. Shi, A. Zieseniss, C.M. Siemssen, K. Dettmer, S. Brodesser, M. Schmidtendorf, J. Lee, H. Wu, C.M. Furdui, S. Brandenburg, J. R. Burgoyne, I. Bogeski, J. Riemer, A. Chowdhury, P. Rehling, T. Bruegmann, V. V. Belousov, D.M. Katschinski, IDH3gamma functions as a redox switch regulating mitochondrial energy metabolism and contractility in the heart, Nat. Commun. 14 (1) (2023) 2123.
[35] B. Steinhorn, A. Sorrentino, S. Badole, Y. Bogdanova, V. Belousov, T. Michel, Chemogenetic generation of hydrogen peroxide in the heart induces severe cardiac dysfunction, Nat. Commun. 9 (1) (2018) 4044.
[36] A. Sorrentino, B. Steinhorn, L. Troncone, S.S.S. Saravi, S. Badole, E. Eroglu, M. F. Kijewski, S. Divakaran, M. Di Carli, T. Michel, Reversal of heart failure in a chemogenetic model of persistent cardiac redox stress, Am. J. Physiol. Heart Circ. Physiol. 317 (3) (2019) H617–H626.
[37] F. Spyropoulos, A. Sorrentino, J. van der Reest, P. Yang, M. Waldeck-Weiermair, B. Steinhorn, E. Eroglu, S.S. Saeedi Saravi, P. Yu, M. Haigis, H. Christou, T. Michel, Metabolomic and transcriptomic signatures of chemogenetic heart failure, Am. J. Physiol. Heart Circ. Physiol. 322 (3) (2022) H451–H465.
[38] P.J. Halvey, J.M. Hansen, J.M. Johnson, Y.M. Go, A. Samali, D.P. Jones, Selective oxidative stress in cell nuclei by nuclear-targeted D-amino acid oxidase, Antioxidants Redox Signal. 9 (7) (2007) 807–816.
[39] B. Chance, H. Sies, A. Boveris, Hydroperoxide metabolism in mammalian organs, Physiol. Rev. 59 (3) (1979) 527–605.
[40] M.P. Murphy, How mitochondria produce reactive oxygen species, Biochem. J. 417 (1) (2009) 1–13.
[41] E. Rosini, L. Pollegioni, S. Ghisla, R. Orru, G. Molla, Optimization of D-amino acid oxidase for low substrate concentrations–towards a cancer enzyme therapy, FEBS J. 276 (17) (2009) 4921–4932.
[42] T. Hatanaka, W. Huang, T. Nakanishi, C.C. Bridges, S.B. Smith, P.D. Prasad, M. E. Ganapathy, V. Ganapathy, Transport of D-serine via the amino acid transporter ATB(0,+) expressed in the colon, Biochem. Biophys. Res. Commun. 291 (2) (2002) 291–295.
[43] J.K. Salabei, A.A. Gibb, B.G. Hill, Comprehensive measurement of respiratory activity in permeabilized cells using extracellular flux analysis, Nat. Protoc. 9 (2) (2014) 421–438.
[44] K.B. Beckman, B.N. Ames, Mitochondrial aging: open questions, Ann. N. Y. Acad. Sci. 854 (1998) 118–127.
[45] R.L. Goncalves, C.L. Quinlan, I.V. Perevoshchikova, M. Hey-Mogensen, M. D. Brand, Sites of superoxide and hydrogen peroxide production by muscle mitochondria assessed ex vivo under conditions mimicking rest and exercise, J. Biol. Chem. 290 (1) (2015) 209–227.
[46] A.P. Kudin, N.Y. Bimpong-Buta, S. Vielhaber, C.E. Elger, W.S. Kunz, Characterization of superoxide-producing sites in isolated brain mitochondria, J. Biol. Chem. 279 (6) (2004) 4127–4135.
[47] J. St-Pierre, J.A. Buckingham, S.J. Roebuck, M.D. Brand, Topology of superoxide production from different sites in the mitochondrial electron transport chain, J. Biol. Chem. 277 (47) (2002) 44784–44790.
[48] M.D. Brand, Mitochondrial generation of superoxide and hydrogen peroxide as the source of mitochondrial redox signaling, Free Radic. Biol. Med. 100 (2016) 14–31.
[49] V. Cracan, D.V. Titov, H. Shen, Z. Grabarek, V.K. Mootha, A genetically encoded tool for manipulation of NADP(+)/NADPH in living cells, Nat. Chem. Biol. 13 (10) (2017) 1088–1095.
[50] J.B. Lim, H.D. Sikes, Use of a genetically encoded hydrogen peroxide sensor for whole cell screening of enzyme activity, Protein Eng. Des. Sel. 28 (3) (2015) 79–83.
[51] T. Shi, D.M.K. van Soest, P.E. Polderman, B.M.T. Burgering, T.B. Dansen, DNA damage and oxidant stress activate p53 through differential upstream signaling pathways, Free Radic. Biol. Med. 172 (2021) 298–311.
[52] D.M.K.v. Soest, P.E. Polderman, W.T.F.d. Toom, S. Zwakenberg, S.d. Henau, B.M. T. Burgering, T.B. Dansen, Mitochondrial H_2O_2 release does not directly cause genomic DNA damage, bioRxiv (2023) 2023, 03.29.534749.